Journal of Catalysis **188,** 176–185 (1999)
Article ID jcat.1999.2636, available online at http://www.idealibrary.com on IDEAL®

FTIR Study of the Low-Temperature Water–Gas Shift Reaction on Au/Fe_2O_3 and Au/TiO_2 Catalysts

F. Boccuzzi,*,[1] A. Chiorino,* M. Manzoli,* D. Andreeva,† and T. Tabakova†

*Dipartimento di Chimica IFM, Università degli Studi di Torino, Via P. Giuria 7, 10125 Torino, Italy; and †Institute of Catalysis, Bulgarian Academy of Sciences, 1113 Sofia, Bulgaria

Received May 10, 1999; revised July 10, 1999; accepted July 12, 1999

An FTIR and quadrupole mass spectroscopic study of the water–gas shift (WGS), the reverse WGS reactions, and the adsorption of the individual molecules involved has been carried out on Au/Fe_2O_3 and Au/TiO_2 catalysts. The chemisorptions and the reactions on the two catalysts have been compared with the aim of gaining a better understanding of the role played by the two phases present in these catalysts and of the synergistic interplay between them in gold catalysts tested for a low-temperature water–gas shift reaction. Evidences are reported that H_2 is dissociated already at room temperature on both the catalysts on gold sites, giving rise to hydrogen atoms that can react with adsorbed oxygen atoms or spillover on the supports where they can reduce the support surface sites. It is shown that CO is adsorbed molecularly on different surface sites, on the support cations, on Au^0 sites exposed at the surface of small three-dimensional particles and also on $Au^{\delta-}$ sites exposed at the surface of negatively charged clusters. The CO formed in the reverse WGS reaction appears chemisorbed only on the Au^0 sites. The support sites and the $Au^{\delta-}$ sites, where the CO appears as more strongly bonded, are present but not accessible to the CO formed by CO_2 reduction, probably because these sites are covered by water. Water and OH groups are adsorbed on the supports, on gold sites, and at the interface between them. The effects of CO coadsorption on water dissociation and of H_2 dissociation on CO_2 reduction have been evidenced. The close similarity of the catalytic activity of the two examined samples indicates that the active sites for hydrogen dissociation and for water–CO reactive interactions are located at the surface of the metallic gold small particles where the reaction can take place by a red–ox regenerative mechanism.

Key Words: **gold catalysts; WGS reaction; FTIR and quadrupole mass study.**

1. INTRODUCTION

The great interest shown in recent years in gold-containing catalysts (1) is justified mainly by the high catalytic activity at low temperatures in a number of important reactions. Recently (2), it was shown that Au/Fe_2O_3 and Au/TiO_2 catalysts, in spite of the very different activity of the two supports in the title reaction, high at high temperature for Fe_2O_3 and almost nil in all conditions for TiO_2, exhibit almost the same activity and also an activity similar to that of the Cu/ZnO catalysts in the water–gas shift (WGS) reaction. The Fe_2O_3- and ZnO-based catalytic systems have been the object of many studies (3, 4). The WGS reaction is thought to occur mainly through two reaction mechanisms, the regenerative, red–ox mechanism and the associative mechanism. The regenerative mechanism involves successive oxidation and reduction of the surface, while the associative mechanism involves reaction through an adsorbed surface intermediate, as a formate mechanism. The possibility of participation of carbonate and bicarbonate intermediate complexes instead of the formates is also under discussion. In the formate mechanism, H_2O dissociates to form OH_a, which then reacts with CO to produce $HCOO_a$. Decomposition of formate then results in H_2 and CO_2 products. In the red–ox mechanism H_2O dissociates completely to O_a and H_a and the O_a is then titrated by CO. Over Fe_3O_4 the regenerative mechanism is thought to be dominant; on many other oxides the associative mechanism is thought to be more important.

In the biphasic catalysts, as the metals supported on the oxides, many studies have been made (5) to understand the role and the synergetic effect of the two phases in the catalytic reaction. Recently (6, 7), kinetic models of the gas shift reaction based on a description of its elementary steps at the atomic level have been presented. The models have been successfully tested against kinetic data for single-crystal surfaces and for working Cu-based catalysts, Cu/ZnO and Cu/Fe_2O_3. The models are based on a statistical mechanical treatment of the red–ox mechanism; in the model formulations the adsorbate–adsorbate interactions were neglected. From this analysis it appeared that the active area of the catalyst is mainly the Cu(111) area and that under most reaction conditions the coverage by the reaction intermediate is small.

On the model catalyst, i.e., vapour-deposited Cu thin films on ZnO single-crystal planes (8), it was shown that

[1] To whom correspondence should be addressed. Fax: +39011 6707855. E-mail: Boccuzzi@ch.unito.it.

0021-9517/99 $30.00

submonolayer Cu films form two-dimensional (2D) metallic islands on which CO adsorbs and desorbs much like those on the Cu(110) surface of bulk Cu, while at higher Cu coverages or after annealing at high temperatures the thickness of the Cu clusters increases and converts the surface to Cu(111) sites. On submonolayer films it was also shown that water and oxygen adsorb like on the Cu(110) surface; after annealing at high temperatures the adsorption is similar to that of Cu(111) surfaces. Moreover, even at high Cu coverages, it was evidenced that water adsorption on ZnO sites, to some extent, was electronically affected by nearby Cu. The Cu has a possibility for electronically influencing the interaction of water with the support in several ways. Moreover, as discussed in the very recent paper previously quoted (7), in reducing conditions Cu–Zn surface alloys can be formed. Similar effects could occur also in other metal–semiconductor oxides systems and justify some peculiar behaviours of these samples.

Recently, some of us (9) studied by FTIR the CO chemisorption and reactivity with oxygen on Cu/ZnO, Cu/TiO_2, Au/ZnO, and Au/TiO_2 and a close similarity was found in the behaviour of the copper and gold catalysts. Up to now there are no FTIR studies concerning the WGS reaction mechanism on gold-supported catalysts.

Here, we will present a FTIR study of the chemisorption, of the mutual interactions, and of the reactivity of the molecules involved in the direct and inverse WGS reaction, namely, CO, H_2O, H_2, and CO_2 on Au/TiO_2 and Au/Fe_2O_3 at different temperatures, from room temperature (RT) up to 523 K, to understand why the two samples have the same activity in the WGS reaction in spite of the very different activity of the two supports and if gold metallic particles play, in these catalysts, the role played by the copper in the copper-containing catalysts. Similar experiments have also been made on the supports to put in evidence, with the same experimental setup and in the same conditions, the effects produced by the gold on the phase transformations, chemisorption, and reactivity of the supports in different atmospheres. We recall here that two different schemes for the WGS reaction on Au/Fe_2O_3 and on Au/TiO_2 were proposed previously by some of us (2). The essential aspects of the mechanism on Au/Fe_2O_3 are the dissociative adsorption of water on ultrafine gold particles, followed by spillover of active hydroxyl groups onto adjacent sites on the ferric oxide and the successive reoxidation of $Fe^{2+} \rightarrow Fe^{3+}$. On Au/TiO_2 it was proposed that the adsorption of CO onto gold particles would be more probable.

2. EXPERIMENTAL

2.1. Materials

The samples were prepared by the deposition–precipitation method in a "Contalab" laboratory reactor (Contraves AG, Switzerland) under complete control of all parameters (2): temperature, pH, stirrer speed, and reactant feed flow rates. All the chemicals used were "analytical grade." The following conditions were employed: 333 K; stirrer speed $= 250$ rpm; reactant flow rate $= 8$ ml/min. The iron hydroxide was prepared by precipitation of iron nitrate with Na_2CO_3 at 333 K. The Au/Fe_2O_3 was prepared by the deposition–precipitation method on freshly prepared iron hydroxide, starting from gold tetrachloric acid. The anatase was prepared by hydrolysis of $TiCl_4$ with ammonia at pH 9, at low temperature. The Au/TiO_2 sample was prepared by deposition–precipitation on a TiO_2 anatase sample. The samples contained 3 wt% Au; before the experiments the samples have been calcined at 673 K and, in some cases that will be specified, reduced at 523 K.

2.2. Methods

The BET area of the samples was determined on a "Flow Sorb II-2300" device. It was found that the area is 66.5 m^2/g for Au/Fe_2O_3 and 86.2 m^2/g for the Au/TiO_2 sample; the Fe_2O_3 area is 65 m^2/g and the TiO_2 area is 90 m^2/g.

X-ray diffraction samples were prepared by means of Synocryl 9122X in a diluted toluene solution and exposed for 6 h in a Guinier-De Wolff-Nonius camera Mark IV, using Fe$K\alpha$1 radiation. The gold–iron oxide sample shows the diffraction peaks of pure hematite on the calcined sample and of pure magnetite after reduction or exposure to the reaction mixture. Transmission electron microscopy (TEM) characterisation was performed on a Hitachi-H-600-2 electron microscope. The average particle size of Au for the two samples is 3–4 nm and does not change appreciably after catalytic tests.

The FTIR spectra have been taken on a Perkin-Elmer 2000 spectrometer, with the samples in self-supporting pellets pressed at 4×10^3 kg/cm^2 and introduced in an AABSPEC cell, allowing to run the spectra in controlled atmospheres and controlled temperatures (from 300 to 800 K). The cell was permanently connected through a needle valve to a VG Micromass spectrometer, to obtain the analysis of the gas phase during the reaction.

3. RESULTS AND DISCUSSION

3.1. FTIR Spectra of CO and CO_2 Adsorption

By adsorption of CO at RT at full coverage on both the oxidised Au/TiO_2 and Au/Fe_2O_3 catalysts (Figs. 1a and 1b, thin curves) bands have been detected at 2110 cm^{-1}, easily assigned on the basis of previous works (9, 10) to the CO chemisorption on Au^0 metallic particles, and at 2170–2190 cm^{-1}, attributed to CO adsorbed on the Ti^{4+} cations (11). Moreover, *bands in the 2050- to 1950-cm^{-1} range* have been observed on prereduced samples (Figs. 1c and 1d, thin curves). Bands in these spectral regions were *never*

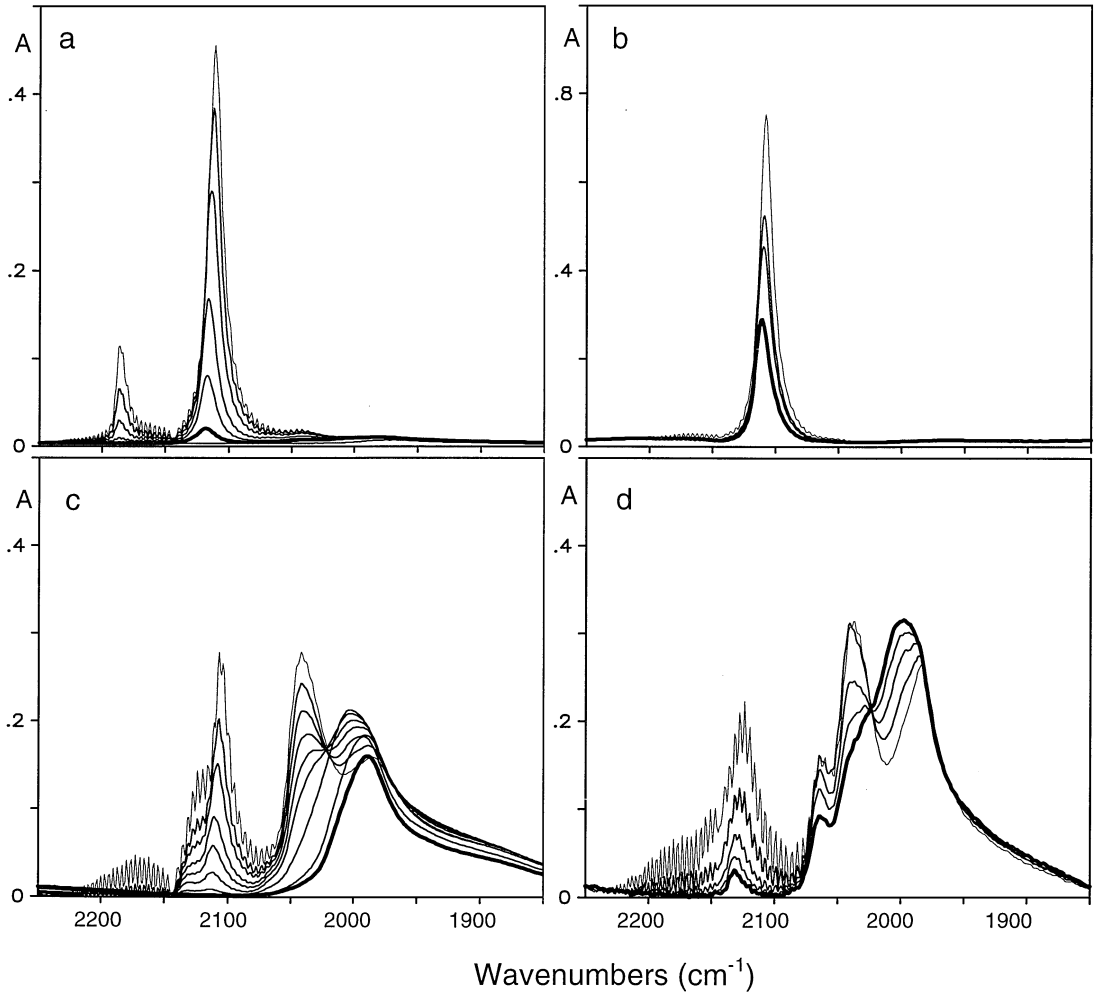

FIG. 1. FTIR spectra in the carbonyl region obtained by CO interaction on (a) oxidised Au/TiO_2, (b) oxidised Au/Fe_2O_3, (c) reduced Au/TiO_2, and (d) reduced Au/Fe_2O_3. CO equilibrium pressures from 20 mbar (thin upper curves) to $\leq$1 mbar (bold lower curves).

detected in previous works concerning $CO–O_2$ reaction over gold-supported catalysts (9, 12) not preliminary reduced, whereas in these studies bands have been sometimes observed at higher frequencies, 2130–2180 cm^{-1}, and assigned to gold sites positively charged or made electropositive by the interaction with the oxidic support.

Bands in the 2050- to 1950-cm^{-1} range are reported in the literature on gold electrodes during the electrooxidation of CO at negative potentials (13). On this basis the bands can therefore be tentatively assigned to CO adsorbed on very small gold clusters, negatively charged as a consequence of an electron transfer from the reduced supports to the small clusters. As it appears evident these bands are quite strong and resistant to the outgassing. When the CO pressure is decreased, the 2110-cm^{-1} band, assigned to the CO chemisorption on Au^0 metallic particles, and the bands at 2170–2190 cm^{-1}, attributed to CO adsorbed on the support cations, smoothly reduce their intensities in the way already discussed in previous papers, while the bands at 2050–1950 cm^{-1} exhibit on both the supports a different and interesting behaviour: the band at 2055 cm^{-1} reduces its intensity while the band at 1990 cm^{-1} grows up and an isosbestic point is evident at about 2015 cm^{-1}. It can be proposed that, with a decrease in the CO coverage, a decrease of the CO adsorbed linearly on top of the small clusters occurs (band at 2055 cm^{-1}) and CO bridge bonded grows up (band at 1990 cm^{-1}). Probably, the electrons transferred from the support to these small clusters allow a back donation from the gold to the carbon monoxide, and a bridge-bonded configuration is stabilized at low coverages. It appears also evident that the CO adsorbed on these sites is more strongly bonded than CO adsorbed on the other, larger gold particles.

A relationship between the WGS activity of metal-supported catalysts and the heat of carbon monoxide adsorption was postulated by Grenoble *et al.* (14). For metals that chemisorb CO weakly, as the gold, the activity was postulated to be low because the concentration of CO–*M* species is low. The optimum strength of CO chemisorption on metals to be active in the WGS reaction appeared to be

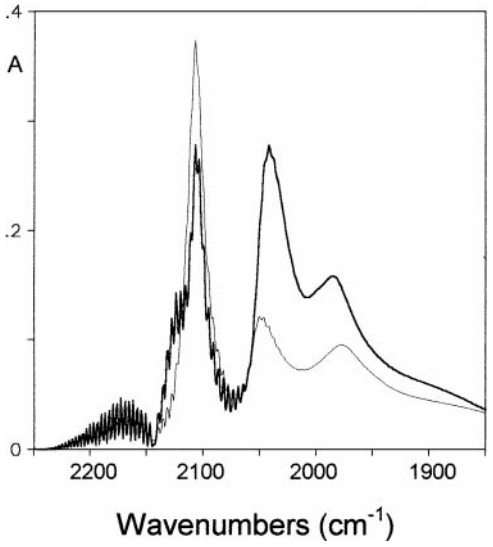

FIG. 2. FTIR spectra in the carbonyl region of the Au/TiO_2 reduced sample contacted with 60 mbar CO (bold curve) and of the same sample previously contacted with 1 mbar O_2 for 2 h at RT and then exposed to 60 mbar CO (thin curve).

near 20 kcal/mol. The strength of the Au–CO bond of the species formed on the small clusters, partially irreversible by outgassing at RT, is in this energy range. However, we will discuss in the last sections the eventual role in the reaction mechanism of the different species put in evidence in the adsorption experiments.

Another interesting feature of these bands is their behaviour with oxygen exposure at room temperature. Figure 2 shows a comparison between the absorption spectra of CO adsorbed on a H_2 reduced Au/TiO_2 sample with the spectrum obtained after the CO inlet on the same reduced sample after outgassing of previous CO and after exposure to O_2 at RT. It appears evident that after oxygen interaction the 2050- and 1990-cm^{-1} bands reduce their intensity while the 2110-cm^{-1} one grows up (thin curve).

Figure 3 shows the effect of the oxygen inlet on CO preadsorbed on the Au/TiO_2 reduced sample. Before the oxygen inlet the main difference in respect to the spectrum shown in Figs. 1c and 2 is the presence of a new shoulder at 1960 cm^{-1}. In the first time (Fig. 3a, curve 2) the 2110-cm^{-1} band reduces its intensity and appears to some extent blue shifted, up to 2116 cm^{-1}; the two low-frequency components, at 2003 and at 1960 cm^{-1}, are almost completely depleted, while the 2050-cm^{-1} band exhibits a small increase in its intensity. At increasing contact times (curves 3–5) minor changes are observed at 2116 cm^{-1}, whereas both the band of the CO chemisorbed on the support and that at 2050 cm^{-1} strongly reduce their intensity.

Valden *et al.* (15) have presented on a model Au/TiO_2 (110) sample evidence by STM/STS (scanning tunnelling microscopy/spectroscopy) of gold clusters with nonmetallic properties when one dimension of the cluster becomes one- or two-atomic-layer thick. Moreover, significant changes in the morphology of the sample were observed on this model catalyst after exposure to O_2 or to an O_2–CO mixture, and the gold cluster density appeared greatly reduced, as a result of a the coalescence of the smaller clusters in the larger particles. In addition, in the same conditions in the XPS spectra a shoulder related to the presence of Ti^{3+} species was completely depleted.

We can hypothesise that in the sample objects of this work a fraction of the deposited gold is formed by very thin gold clusters, covered at the end of the calcination by adsorbed oxygen. By reduction in H_2 at 523 K both oxygen adsorbed on gold clusters and a fraction of the oxygen at the surface of titania or of the iron oxide are reduced and an electron transfer from the reduced supports to the gold

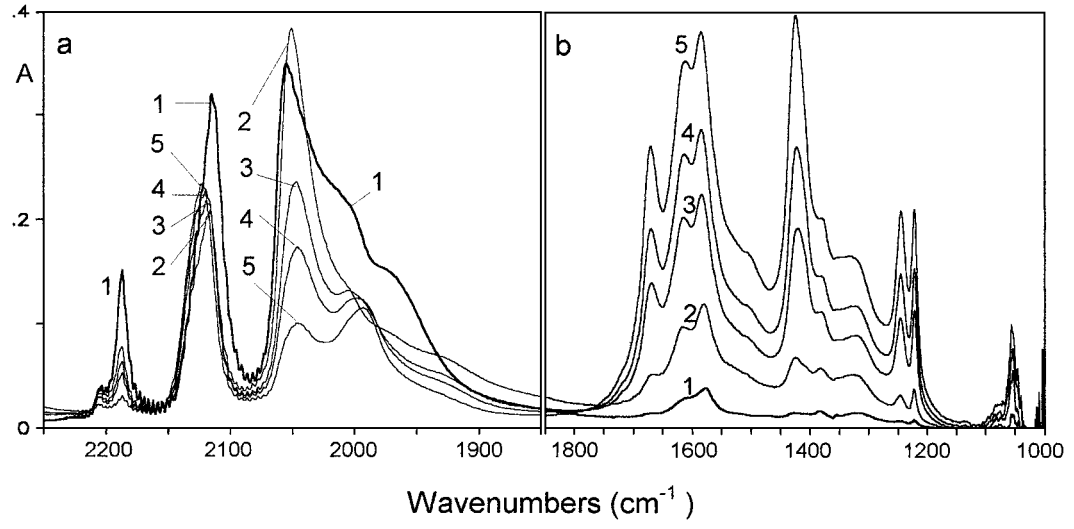

FIG. 3. FTIR spectra in the carbonyl region (section a) and in the carbonate region (section b) obtained by O_2 interaction on a Au/TiO_2 reduced sample precovered with CO: curve 1, 20 mbar CO; curves 2–5, effect of 5 mbar O_2 admission immediately, after 3, 5, and 10 min, respectively.

particles and to the small gold clusters takes place. On the very small clusters the negative charge can produce a significant effect on the chemical properties of the exposed sites, giving rise, by interaction with CO, to bands red-shifted and more resistant to the outgassing than on the larger particles, where the negative charge must be distributed on a large number of atoms and is mainly localised at the interface between the support and the metal. Bands in this region have also been observed on a sample already used in the reactor, exposed to the air and put in the spectroscopic cell without any preliminary activation procedure (spectra not shown for the sake of brevity). On the contrary, the exposure to pure oxygen in clean, controlled conditions at RT irreversibly reduces the intensity of these bands (Fig. 2). Probably, by interaction with pure oxygen at RT, the negative charge is transferred to the oxygen species adsorbed at the surface of the catalysts, as a consequence of their high electronegativity, and the small gold clusters coalesce in the larger particles, irreversibly.

At the same time a significant increase of bands in the region of the carbonate and bicarbonate species adsorbed on the support is observed: their intensity, at the end of the interaction, appears similar to that of the carbonylic bands on the gold small clusters. On the oxidised sample the intensity of these bands is significantly weaker (Fig. 4, curve 1), as they were also very weak in the previously examined sample (Ref. 9b, Fig. 5). It can be hypothesised that the

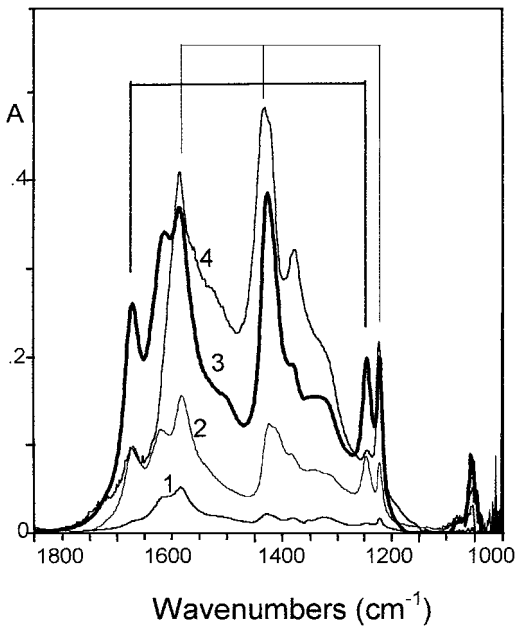

FIG. 4. FTIR spectra of Au/TiO_2 in the carbonate region, obtained by different treatments: curve 1, 20 mbar CO on an oxidised sample; curve 2, 60 mbar CO on a reduced sample, previously contacted with 1 mbar O_2 for 2 h at RT; curve 3, 5 mbar O_2 for 10 min on a reduced sample precovered with CO (as curve 5 on Fig. 3b); curve 4, 10 mbar CO_2 on an oxidised sample.

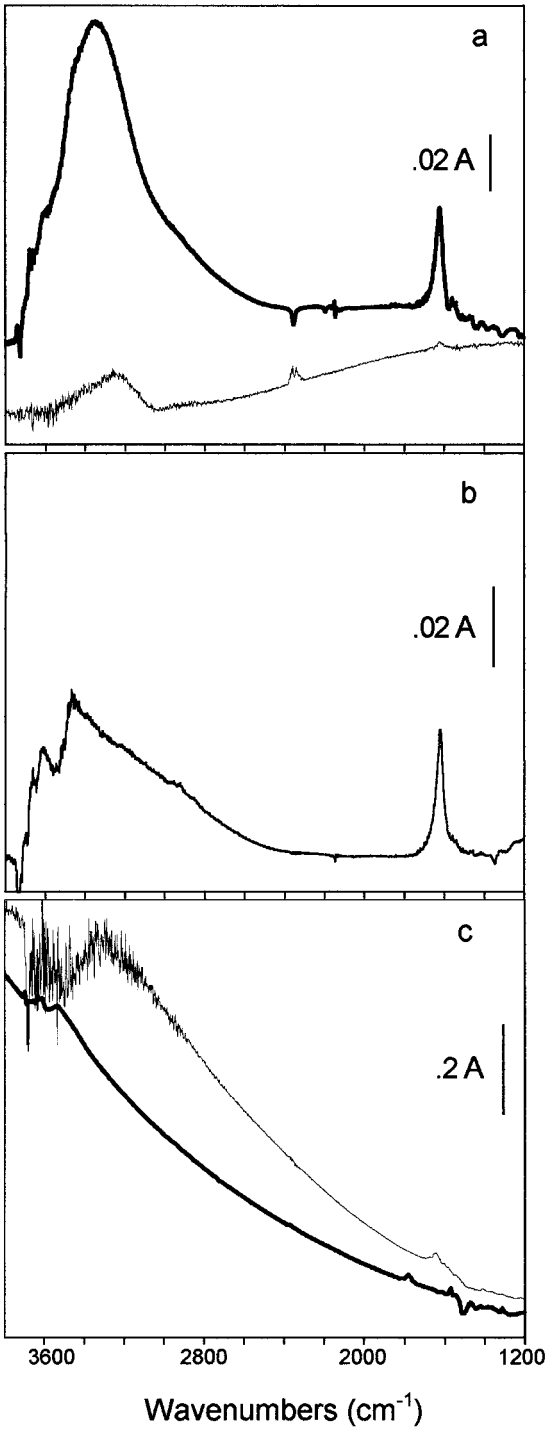

FIG. 5. (Section a) Effect of hydrogen admission on the FTIR spectrum of oxidised (bold curve, 20 mbar) and reduced Au/TiO_2 (thin curve, 5 mbar). (Section b) Effect of water admission (3×10^{-2} mbar) on the FTIR spectrum of oxidised Au/TiO_2. (Section c) Effect of hydrogen admission at RT on the FTIR spectrum of oxidised Au/Fe_2O_3 (thin curve, 10 mbar) compared with the effect of heating in hydrogen at 523 K on the FTIR spectrum of Fe_2O_3 (bold curve, 20 mbar).

oxygen atoms adsorbed on gold small clusters have a quite strong Bronsted base strength and nucleophilic character or that they induce an increase in the reactivity of the oxygen atoms of the support. At the end of the interaction bands are evident at 1582, 1413, and 1220 cm^{-1}, assigned to a bicarbonate species (9b) adsorbed on the support together with two additional, quite sharp bands at 1670 and 1243 cm^{-1}, that on the basis of their greater intensity on the prereduced sample and taking in account previous assignments of similar features made by Ramis *et al*. (16), can be ascribed to the asymmetric and symmetric stretching frequencies of a side-on bent CO_2^- carboxylate species adsorbed on Ti^{3+} sites, in close contact with the gold small clusters.

CO_2 adsorption produces on Au/TiO_2 and on Au/Fe_2O_3 (not shown for sake of brevity) a band strongly dependent on the pressure at 2351 cm^{-1} and two much weaker bands at 2383 and 2285 cm^{-1} that can be easily assigned, on the basis of literature data (16), to CO_2 molecules linearly adsorbed on top on the surface cations of support terraces, on step sites, and to $^{13}CO_2$, respectively. Moreover different bands grow up in the carbonate-like region. The comparison reported in Fig. 4, between the spectra observed in the carbonate-like region, shows that the CO_2 interaction on the oxidised sample produces bicarbonate species of intensity quite similar to those produced by oxygen interaction on CO preadsorbed on the reduced one, whereas the bands assigned to the side-on bent CO_2^- species are significantly weaker.

3.2. *Hydrogen and Water Adsorption*

The hydrogen interaction at RT on the oxidised Au/TiO_2 catalysts produces a broad band in the OH stretching region with a maximum at $\approx$3300 cm^{-1} and FWHM $\approx$ 400 cm^{-1} (Fig. 5a, bold curve) whose intensity grows up with the H_2 pressure and the contact times. On the high-frequency side of the band also two weak narrow shoulders at 3662 and 3612 cm^{-1} are evident while from the low-frequency side another broad shoulder is observed, at $\approx$3000 cm^{-1}. Finally, a weak band is detected at 1620 cm^{-1} in the region typical of the water molecule bending. It can be concluded that hydrogen is dissociated on the gold particles and that the hydrogen atoms react with adsorbed oxygen species.

The hydrogen interaction at RT on a reduced Au/TiO_2 sample (Fig. 5a, thin curve) causes a monotonous increase in the absorbance of the sample, maximum at low wavenumbers, a band at 3300 cm^{-1}, weaker than in the case of the oxidised sample and without the higher frequency shoulder. Moreover, more important, almost no bands in the water-bending region are detected. We recall that, on TiO_2 alone, H_2 interaction at RT does not produce any spectroscopic effect; an absorbance increase is observed only by heating up to 423 K. Water absorption on TiO_2 (11) produces a quite complex spectrum, characterised by several components.

Monotonous absorbance increases have been observed on Pt/TiO_2 and other transition metal supported catalysts by H_2 interactions at RT (17) and ascribed to the population of Ti^{3+} shallow donor levels, as a consequence of the spillover of hydrogen atoms from the metal particles to the surface of the oxide, where they are adsorbed in a protonic form. On pure TiO_2 a higher temperature is needed to activate the hydrogen molecules. Gold is usually considered inactive in the H_2 dissociation; however, it must be considered that small gold particles and clusters may show an unusual, higher activity.

As for the absorption bands in the OH mode regions, it appears evident that the hydrogen produces an absorption significantly stronger and less structured in respect to that produced by the inlet of small doses of water on the Au/TiO_2 oxidised sample (Fig. 5b) and with the maximum at a lower frequency. Moreover, water adsorption on an oxidised sample produces a well-defined negative band at 3731 cm^{-1}, almost absent after hydrogen adsorption. The absence of the negative band in the absorption produced by hydrogen interaction appears as an indication that the OH species formed by the H_2 inlet do not make hydrogen bond interactions with the OH groups of the support. However, the most important difference is that the intensity ratio between the bending mode of the water and the absorption in the OH stretching region is much lower after H_2 interaction on the oxidised sample than after H_2O interaction and that the water-bending mode is completely absent after H_2 interaction on the Au/TiO_2 reduced sample.

The intensity ratio between different vibrational modes of the same molecule can change if the molecule is adsorbed on a metallic surface: the vibrational modes with the oscillating dipole moment parallel to the metallic surface are depleted while those with the dipole moment perpendicular to the metallic surface are intensified as a consequence of the "metallic surface IR selection rule." If the water molecules formed by H_2 interaction are adsorbed on the metallic gold with their molecular plane perpendicular to the metallic surface, the depletion of the bending mode can be justified. However, this arrangement is ideal and quite unrealistic. Synchrotron infrared spectra of H_2O adsorbed on a polycrystalline gold surface (18) showed a broad absorption at 3387 cm^{-1}, at a frequency which is significantly lower than that for isolated water molecules absorbing at about 3600 cm^{-1}, indicative of hydrogen-bonded surface water and a weak band at 1663 cm^{-1}, characteristic of the H–O–H bending mode, and significantly blue-shifted in respect to the 1620 cm^{-1} bending frequency of isolated water molecules.

However, another explanation of the lower intensity ratio between the stretching and bending region can be proposed: by H_2 interaction on samples pretreated with O_2, OH groups are formed instead of water molecules. The activity of O_{ads} for hydrogen dissociation or abstraction from

water molecules has been observed in many cases (19) and it appears to be independent of the metal and of the coverage. On Cu, Ag, Pd, and Ni it is greatest for low coverages of O_{ads}, 0.1–0.25 monolayers usually. The activity of different oxygen adsorbed species was shown to be to some extent related to the degree of coordinative insaturation. It appears likely that, on bulk metals, the reaction of OH formation occurs at the edges of oxygen islands; in the case of supported metals probably the most reactive sites are at the interface between the metal and the support. In the absence of oxygen-reactive species, as shown in Fig. 5a, thin curve, the OH spectroscopic features produced by hydrogen interaction are significantly weaker.

The hydrogen interaction at RT on oxidised Au/Fe_2O_3 causes a strong increase in the IR absorbance at high frequencies (Fig. 5c, thin curve), similar to that produced by reduction of Fe_2O_3 at 523 K (Fig. 5c, bold curve), while the effect of H_2 on Fe_2O_3 at RT is almost nil (not shown for sake of brevity). The different behaviours of gold-containing samples in respect to the support alone confirm that also in this case gold particles are able to dissociate hydrogen molecules. On Au/Fe_2O_3 the atomic hydrogen atoms cause the reduction of some Fe^{3+} ions to Fe^{2+} ions, giving rise to a magnetite-like surface phase. The optical band gap of Fe_3O_4 is 0.3 eV, i.e., $\approx$2500 cm^{-1} (20), where a strong increase in the IR absorbance is observed. As confirmation of this spectroscopic finding, we recall here that it was shown by some of us (21) by TPR data that gold influences the reduction of Fe_2O_3 to Fe_3O_4, shifting the bulk reduction temperature from 700 to 553 K.

3.3. *FTIR Study of the WGS CO–H_2O Reaction*

The inlet of water on preadsorbed CO on the Au/TiO_2 reduced sample already at RT produces CO_2, bicarbonates (Fig. 6a, curves 2–4) and changes in the carbonylic region (Fig. 6a, inset). The main changes in the carbonylic region are (i) the rapid decrease of the bands at 2180–2200 cm^{-1} assigned to CO adsorbed on Ti^{4+} surface cations, (ii) a gradual reduction of the intensity of the 2110- and 2030-cm^{-1} bands, assigned to CO adsorbed on top of gold sites exposed at the surface of gold particles and on gold negatively charged clusters, respectively, (iii) the intensification of the 1990-cm^{-1} band, assigned to CO bridge bonded on gold negatively charged clusters. Moreover, almost immediately a band is depleted at 1940 cm^{-1}, which we still have not assigned yet, probably due to the CO adsorption on negatively charged gold clusters of smaller sizes and/or higher negative charges of those previously mentioned. The decrease of the bands assigned to CO adsorbed on Ti^{4+} surface cations is due to the displacement of the adsorbed CO by water molecules that can be adsorbed molecularly on these sites.

The 2110-cm^{-1} band decrease appears directly related to the CO_2 formation, while the decrease of the 2030-cm^{-1} band appears related to the intensification of the 1990-cm^{-1} band. It appears, from these spectroscopic data, that water acts as an oxygen-donating coreactant on the small gold particles while it induces a change in the CO coordination, from on top to bridge bonded, on the negatively charged gold clusters. When the temperature is increased upto 523 K, almost all the vibrational bands previously illustrated are depleted (Fig. 6a, curve 5). In the high-frequency range two weak bands are present, at 2930 and 2851 cm^{-1}, observed already by heating at 373 K, that could be related to the C–H stretching of a formate species produced by bicarbonate decomposition. At low frequencies a monotonous absorption

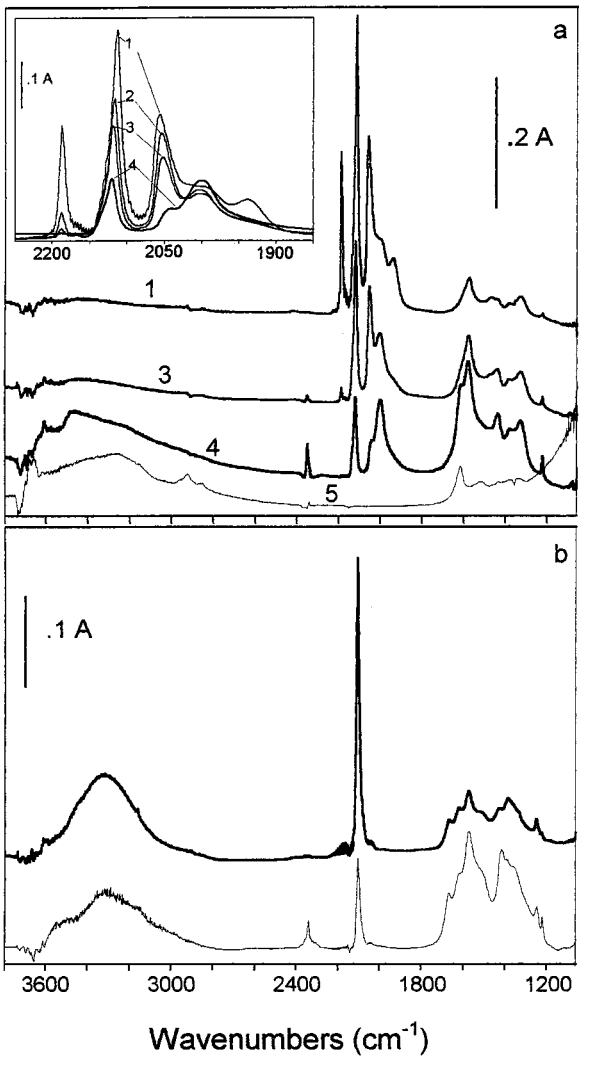

FIG. 6. (Section a) FTIR spectra scanned before and during the WGS reaction performed on reduced Au/TiO_2: curve 1, 25 mbar CO; curve 2, immediately after admission of the first dose of H_2O (3.6×10^{-2} mbar) on the IR sample cell, already containing a much higher CO pressure; curve 3, immediately after admission of the second dose of H_2O (2.5×10^{-1} mbar); curve 4, after 1 h of reaction at RT; curve 5, after 10 min at 250°C. The carbonylic region is magnified in the inset. (Section b) Effect of CO admission on the FTIR spectra of Au/TiO_2 precovered with H_2O, in the presence of the water–vapour phase (thin curve) or in its absence (bold curve).

is evident which can be ascribed to the population of Ti^{3+} donor levels, caused by hydrogen produced in the reaction. The quadrupole mass analysis of the gas phases during this experiment evidenced the presence of significant amounts of H_2 and CO_2 already at 373 K, growing, in agreement with previous catalytic results (2), by increasing the temperature up to 573 K.

Other interesting aspects of the $CO–H_2O$ interaction on the Au/TiO_2 catalyst are put in evidence in the experiments reported in Fig. 6b, where the spectra taken after CO interaction on preadsorbed water are reported, in the presence of water vapour (thin curve) or after outgassing of water vapour (bold curve). The most evident difference between these two spectra is the presence of the CO_2 band when CO is adsorbed in the presence of water vapour. It appears therefore evident that the presence of molecular water is needed to obtain molecular CO_2. This reaction is to some extent preliminary to the WGS one. Moreover, when one looks at the two curves, it appears evident that the CO inlet on water produces in the carbonylic region only one band at the 2110-cm^{-1} band, related to CO adsorbed on small gold metallic particles, while the bands present in the experiments shown in Fig. 6a, assigned to CO adsorbed on surface cations and on negatively charged gold clusters, are completely absent. These sites appear completely saturated by the preadsorbed water. Moreover, in both the experiments, the *CO inlet produces a broad absorption with a maximum at 3320 cm^{-1}, similar in shape to that observed after H_2 interaction (Fig. 5a), which appears related to Au–OH species, produced by reaction of CO with the water*. The frequency and the broad width of the observed features can be taken as an indication that these OH groups are involved in a hydrogen bond of intermediate strength, probably in mutual interaction or in interaction with water or with the oxygen of the support. The water vapour present in the mixture is probably activated by the hydroxyl groups formed on gold, via hydrogen bonding. As in the CO electrooxidation (13) the possible involvement of coadsorbed hydroxyls or related species formed by incipient surface oxidation can be postulated.

These features appear also coherent with the water-catalysed red–ox mechanism proposed by Campbell *et al.* (22) in the study of the WGS reaction on metallic copper. It was proposed that on Cu and possibly on Ag and Au the *water dissociation, rather than CO adsorption, is the rate-limiting step.*

As for the carbonate-like region, the main features of the two experiments reported in Fig. 6b are quite similar, whereas some differences are evident with the spectra reported in Fig. 6a, in particular a lower intensity of the bands assigned to the bicarbonate species and the presence of the bands at 1670 and 1247 cm^{-1}, assigned to the CO_2^- species in Fig. 6b.

CO adsorbed on the Au/Fe_2O_3 sample (Fig. 7, curve 2) immediately produces carbonylic bands in the 2200- to 1950-cm^{-1} range, already discussed, bands in the carbonate-like region at 1620, 1435, 1408, and 1223 cm^{-1}, and a modification in the overall transparency of the sample. The same kind of experiment on Fe_2O_3 produces spectroscopic features significantly different: the carbonate-like species produced are weaker and the overall transparency modification is not observed at all (Fig. 7, curve 1). The inlet of water on the preadsorbed CO produces a broad absorption band in the 2600- to 3600-cm^{-1} range, due to the OH stretching modes of water molecules interacting by hydrogen bonds with surface OH groups, which as a consequence appear as negative bands at 3629 and 3691 cm^{-1}. At increasing contact times (curves 3 and 4) the water-related bands (2600–3600 cm^{-1} and 1620 cm^{-1}) grow up while the carbonylic and bicarbonate bands are depleted. In the carbonate-like region only an isolated band grows up at 1307 cm^{-1}. Moreover, an almost complete loss of the IR transparency is observed already at RT after 3 h of interaction.

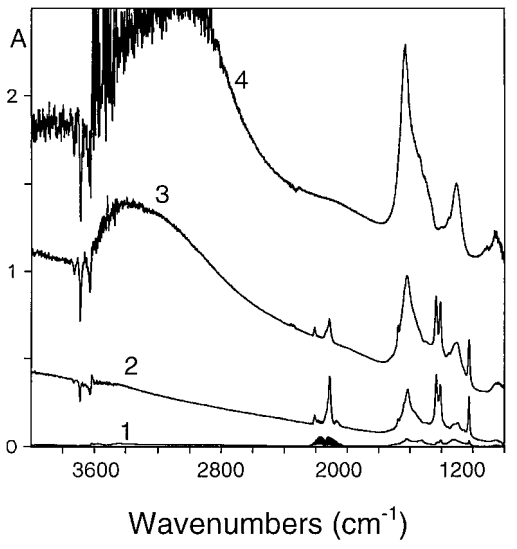

FIG. 7. FTIR spectra scanned before and during the WGS reaction performed on oxidised Au/Fe_2O_3: curve 1, 20 mbar CO on pure Fe_2O_3 for comparison; curve 2, 15 mbar CO on Au/Fe_2O_3; curve 3, immediately after admission of H_2O on the IR sample cell, already containing an equivalent CO pressure; curve 4, after 1 h of reaction at RT.

The changes in the IR transparency observed on the Au/Fe_2O_3 sample, not observed on Fe_2O_3 alone, can be taken, also on the basis of previously illustrated interaction with hydrogen and of the experiments shown on the Au/TiO_2 sample, as indirect evidence of a CO-promoted dissociation of the water on the gold sites, giving rise to the hydrogen formation and to the surface reduction of Fe_2O_3 to Fe_3O_4.

3.4. FTIR Study of the Reverse WGS $CO_2–H_2$ Reaction

FTIR experiments concerning the reverse WGS reaction on the Au/TiO_2 sample are shown in Fig. 8. It appears

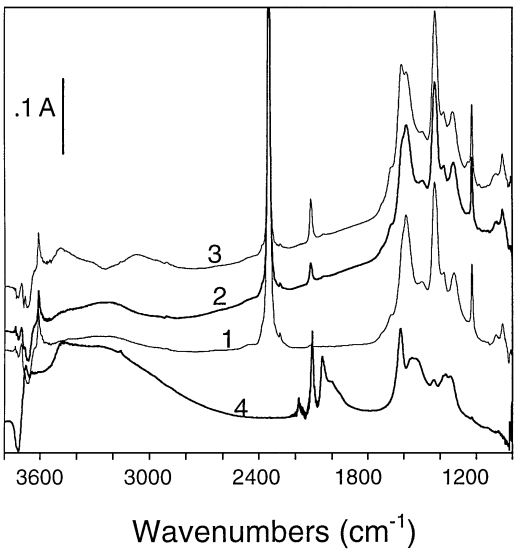

FIG. 8. FTIR spectra scanned during and after the reverse WGS reaction performed on reduced Au/TiO_2: curve 1, immediately after admission of H_2 on the IR sample cell, already containing an equivalent CO_2 pressure; curve 2, after 1 h of reaction at RT; curve 3, after 3 h of reaction at RT; curve 4, admission of CO at the end of the reaction, after outgassing at RT.

evident that already after 1 h of contact (curve 2) a weak band at 2110 cm^{-1}, typical of CO adsorbed on gold particles, together with the strong band of CO_2, weakly adsorbed on the support and with bands due to carbonate and bicarbonate species, are evident. With respect to the spectrum taken immediately before H_2 admission (curve 1), it is evident that the CO band does not appear by contact with CO_2 alone, without hydrogen. Moreover, a monotonous increase in the absorbance in the low-frequency region and an absorption in the OH stretching region become evident. Both these features indicate, as discussed previously, that H_2 is dissociated at the surface of the metallic particles, giving rise to H atoms that can reduce CO_2 molecules with the formation of water and/or Au–OH species. After 3 h of contact the CO band grows up; moreover, two maxima at 3494 and 3070 cm^{-1} are evident in the OH stretching region. The shape and the position of the maximum at higher frequency are similar to those caused by water adsorption and can be assigned to H_2O adsorbed on the support, produced by reaction of hydrogen atoms coming from the dissociation of hydrogen molecules and oxygen atoms produced in the CO_2 decomposition. The maximum at lower frequency is related to Au–OH species, previously discussed in the H_2 section. It appears evident that with an increase in the contact times, the band shifts toward lower frequency, as a consequence of the increase, by increasing the coverage of the hydrogen, of hydrogen bond interactions. After outgassing of the reaction mixture and admission of pure CO (Fig. 8 curve 4), a CO absorption spectrum similar to that observed on the original catalysts is detected. It appears evident that all the sites evidenced by CO are present on the sample at the end of the reaction but some of them are covered by another reaction product, OH or H_2O.

4. CONCLUSIONS

The FTIR study of the adsorption of the molecules involved in the water–gas shift and reverse water–gas shift reactions on Au/Fe_2O_3 and Au/TiO_2 catalysts, of their coadsorptions and their reactive interactions from room temperature up to 523 K showed the following:

—H_2 is dissociated already at room temperature on both the catalysts on gold sites, giving rise to hydrogen atoms that can react with adsorbed oxygen atoms or spillover on the supports where they can reduce the support surface sites.

—CO is adsorbed molecularly on different surface sites, on the support cations, on Au^0 sites exposed at the surface of small three-dimensional particles, and also on $Au^{\delta-}$ sites exposed at the surface of small clusters; however, the *CO formed in the reverse WGS reaction appears chemisorbed only on the Au^0 sites at the surface of small three-dimensional particles*. The other sites and among them $Au^{\delta-}$, where the CO is more strongly bonded, are present but not accessible to the CO formed by CO_2 reduction, probably because they are covered by other reactants or reaction products.

—Water and OH groups are adsorbed on the supports, on gold sites and at the interface between them.

—effects of CO coadsorption on water dissociation and of H_2 dissociation on CO_2 reduction have been evidenced.

In conclusion, the two gold-containing catalysts prepared by supporting the metallic particles on titania, almost completely inactive at any temperature, and on Fe_2O_3, active only at high temperatures, show high and similar low-temperature catalytic activity in the water–gas shift reaction: this high activity appears justified, taking in account that the active sites for hydrogen dissociation and for water–CO reactive interactions are located, on the basis of the experimental finding, at the surface of the metallic gold small particles. A red–ox, regenerative mechanism, similar to that discussed for copper-based catalysts, can explain all the experimental results.

REFERENCES

1. Haruta, M., *Catal. Today* **36**, 153 (1997) and references therein.
2. (a) Andreeva, D., Idakiev, V., Tabakova, T., and Giovanoli, R., *Bulg. Chem. Commun.* **30**, 64 (1998). (b) Andreeva, D., Idakiev, V., Tabakova, T., and Andreev, A., *J. Catal.* **158**, 354 (1996). (c) Andreeva, D., Idakiev, V., Tabakova, T., Andreev, A., and Giovanoli, R., *Appl. Catal. A* **134**, 275 (1996).
3. Rethwich, D. G., and Dumesic, J. A., *Appl. Catal.* **21**, 97 (1986).
4. Rhodes, C., Huchings, G. J., and Ward, A. M., *Catal. Today* **23**, 43 (1995).
5. Campbell, C. T., *Surf. Sci. Rep.* **27**, 1 (1997).
6. Ovesen, C. V., Stolztze, P., Norskov, J. K., and Campbell, C. T., *J. Catal.* **134**, 4445 (1992).

7. Topsoe, N. Y., and Topsoe, H., *J. Mol. Catal. A*, in press.
8. Zhang, C., Ludviksson, A., and Campbell, C. T., *Surf. Sci.* **289**, 1 (1993).
9. (a) Boccuzzi, F., and Chiorino, A., *J. Phys. Chem*. **100**, 3617 (1996). (b) Boccuzzi, F., Chiorino, A., Tsubota, S., and Haruta, M., *J. Phys. Chem*. **100**, 3625 (1996).
10. Ruggiero, C., and Hollins, P., *Surf. Sci.* **377–379**, 583 (1997).
11. Morterra, C., *J. Chem. Soc., Faraday Trans 1* **84**, 1617 (1988).
12. Guillemot, D., Borovkov, V. Yu., Kazansky, V. B., Polisset-Thfoin, M., and Fraissard, J., *J. Chem. Soc., Faraday Trans.* **93**, 3587 (1997).
13. Chang, S. C., Hamelin, A., and Weaver, M. J., *Surf. Sci.* **239**, L543 (1990).
14. Grenoble, D. C., Estadt, M. M., and Ollis, D. F., *J. Catal.* **67**, 90 (1981).
15. Valden, M., Lai, X., and Goodman, D. W., *Science* **281**, 1647 (1998).
16. Ramis, G., Busca, G., and Lorenzelli, V., *Mater. Chem. Phys.* **29**, 425 (1991).
17. Conner, W., Jr., Pajonk, G. M., and Teichner, S. J., *in* "Advances in Catalysis" (D. D. Eley, H. Pines, and P. B. Weisz, Eds.), Vol. 34, p. 1. Academic Press, San Diego, CA, 1986.
18. Melandres, C. A., Beden, B., Bowmaker, G., Liu, C., and Maroni, V. A., *Langmuir* **9**, 1980 (1993).
19. Carley, A. F., Davies, P. R., Roberts, M. W., Shukla, N., Song, Y., and Thomas, K. K., *Appl. Surf. Sci.* **81**, 265 (1994).
20. (a) Balberg, I., and Pankove, J. J., *Phys. Rev. Lett.* **27**, 596 (1971). (b) Hashimoto, T., Yamada, T., and Yoko, T., *J. Appl. Phys.* **80**, 3184 (1996).
21. Ilieva, L., Andreeva, D., and Andreev, A., *Thermochim. Acta* **292**, 169 (1997).
22. Nakamura, J., Campbell, J. M., and Campbell, C. T., *J. Chem. Soc., Faraday Trans.* **86**, 2725 (1990).